

Edge Detection Using Integrate and Fire Neuron Model

M. Ozan İNCETAŞ^{*1}, Rukiye UZUN ARSLAN²

¹Alanya Alaaddin Keykubat University, ALTSO Vocational School, Department of Electric and Energy, 07450, Antalya, Turkey

²Zonguldak Bulent Ecevit University, Engineering Faculty, Department of Electrical & Electronics Engineering, 67100, Zonguldak, Turkey

(Alınış / Received: 27.05.2019, Kabul / Accepted: 30.07.2019, Online Yayınlanma / Published Online: 30.08.2019)

Keywords

Edge detection,
Receptive field,
Spiking neuronal network

Abstract: Edge detection is one of the most basic stages of image processing and have been used in many areas. Its purpose is to determine the pixels formed the objects. Many researchers have aimed to determine objects' edges correctly, like as they are determined by the human eye. In this study, a new edge detection technique based on spiking neural network is proposed. The proposed model has a different receptor structure than the ones found in literature and also does not use gray level values of the pixels in the receptive field directly. Instead, it takes the gray level differences between the pixel in the center of the receptive field and others as input. The model is tested by using BSDS train dataset. Besides, the obtained results are compared with the results calculated by Canny edge detection method.

Topla ve Ateşle Nöron Modeli Kullanılarak Kenar Algılama

Anahtar Kelimeler

Kenar algılama,
Alıcı bölge,
İğnecikli sinir ağları

Özet: Kenar algılama, görüntü işlemenin en temel aşamalarından biridir ve birçok farklı alanda kullanılmaktadır. Kenar belirleme yöntemlerinin amacı görüntüyü oluşturan pikselleri belirlemektir. Çoğu araştırmacı, insan gözünün belirlediği gibi nesnelerin kenarlarını doğru algılamayı hedeflemiştir. Bu çalışmada, iğnecikli sinir ağ yapısına dayalı yeni bir kenar algılama tekniği önerilmiştir. Önerilen model, literatürde bulunanlardan farklı bir alıcı yapısına sahiptir ve doğrudan alıcı alandaki piksellerin gri seviye değerlerini kullanmamaktadır. Bunun yerine, girdi olarak alıcı alanın ortasındaki piksel ile diğerleri arasındaki gri seviye farklarını kullanarak kenar algılama işlemi gerçekleştirilmektedir. Geliştirilen model, BSDS öğrenme veri seti kullanılarak test edilmiştir. Ayrıca, elde edilen sonuçlar Canny kenar algılama yöntemi yardımıyla hesaplananlar ile karşılaştırılmıştır.

1. Introduction

Edge detection is very important operation for the image processing because it is used in many areas such as feature extraction, segmentation, object recognition and image retrieval. Edge detection can be defined as a sudden change between neighboring pixels. There have been improved many approaches based differences and similarities of neighboring pixels in an image [1-3].

Many image processing techniques, including edge detection algorithms, actually aim to reach the perception of the human eye. Human visual system (HVS) has a quite complex process, which starts within the retina and becomes considerably more complex at other stages (the visual pathways and visual cortex) [4-7]. Many researches by neurologist

and computer scientists have been devoted to understand the operation of this complex process and to develop models simulating its behavior [8-13]. In this context, spiking neural networks (SNN) imitate more exactly the biological image processing in HVS. SNNs permit real-time processing which has high speed and computational power due to the usage of temporal coding scheme [14-18]. SNNs use simple neuron models and process the information via encoding by the spikes. In literature, one can find many studies for edge detection based biological neural systems. For example, Wu et al. [19] proposed a network model based on SNNs for edge detection. Meftah et al. [20] developed a SNN model to fulfill segmentation and edge detection. Kerr et al. [21] presented an approach for edge detection using both SNNs and a biologically plausible hexagonal pixel arrangement with hexagonally arranged near-

circular receptive fields. In another study, a bio-inspired model called The Perceptual boundary rEcurrent dEtection Neural (PREEN) in the recurrent interactions of the early visual areas was proposed by Diaz-Pernas et al. [22] to detect color natural scenes boundaries. They concluded that the proposed model gives better results as compared with the best algorithms for some images in Berkeley Segmentation Test Dataset. A computational model, named as COF, is developed for the orientation-selective cell in the primary visual cortex - V1 [23]. In a recent study, Yedjour et al. [18] have proposed a SNN using Hodgkin-Huxley (HH) model for edge detection. They analyzed the performance of the model by using five different edge detection methods. Although it is stated that the model is evaluated with BSDS images and gives more successful results than the classical models, it is seen that the techniques used for comparison are more suitable for the test of noise filters. Most of these aforementioned studies took in consideration the simplified neuron models even though there is a more realistic neuron model (HH model) which simulate the activity of a neuron with a high degree of precision. However, the usage of HH model requires long simulation time, powerful and expensive machines, due to its computational complexity. Because of this, it has been preferred to use simplified neuron models. In this study, we used conductance-based integrate-and-fire (IF) neuron model to detect edges in images.

Remainder of this paper is organized as follows. "Conductance-Based Integrate-and-Fire Neuron Model" section gives a brief introduction to integrate-and-fire neuron model. The architecture of the network is presented in "Network structure" section. The simulation results and discussions are presented in "Simulation results" and "Conclusion" sections, respectively.

2. Material and Method

2.1. Conductance based integrate and fire neuron model

HH model proposed by Hodgkin & Huxley [24] is the first mathematical neuron model, which describes the electrical behavior of neuron excellently. The model uses a set of nonlinear differential equations to characterize how action potential (or spike) is initiated and propagated [18, 25]. However, the usage of this model has some drawbacks; such as, the requirement of solving a set of several first-order differential equations induces that the numerical implementations are computationally expensive and the analysis are difficult. Therefore, in literature, there have been proposed more simple neuron model such as integrate-and-fire (IF), FitzHugh-Nagumo (FHN), Izhikevich neuron models etc. [26-29]. Among these, IF neuron model is the much simplified model and captures many of the principal features of neuron dynamics, thus it is quite popular at discussing of the

neuronal coding, memory or neuron's dynamics [28, 30, 31]. The model is also more useful as compared to HH model, if the model is applied to large-scale neuronal networks in terms of computational complexity [19]. It is well known that the variation of ion channels (Na⁺ and K⁺) conductance at the HH model have vital effects in spike generation [32]. By taking into this consideration, conductance-based IF model was conceived [33].

In the conductance based integrate-and-fire model, the time evolution of the membrane potential ($v(t)$) is given as follows [19, 28, 34-36]:

$$c_m \frac{dv(t)}{dt} = g_l (E_l - v(t)) + \sum_j \frac{w^j g_{syn}^j(t)}{A_{syn}} (E_{syn} - v(t)) \quad (1)$$

Where c_m is the capacitance, g_l represents the conductance and E_l is reversal potential of the membrane, respectively. E_{syn} is the reversal potential of inhibitory (i) and excitatory (e) synapses where $s \in \{i, e\}$, respectively. w^j represents the strength of the synapse j , and the membrane patch area (A_{syn}) is linked to the corresponding synapse. g_{syn}^j represents the conductance of synapse j . If $v(t)$ reaches a certain threshold v_{th} (spiking threshold), it is instantaneously reset to a lower value v_r (reset potential) for a time τ_{ref} (refractory time) and a spike occurs. A neuron receives spike trains from three afferent neurons in a receptive field is given in Figure 1.

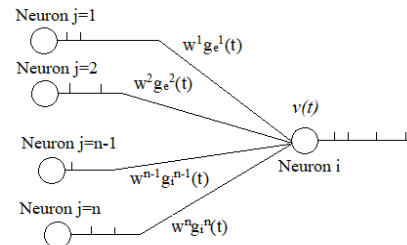


Figure 1. Conductance based synapses connections in a spiking neuron model

2.2. Network structure

Figure 2 shows the preferred network model which is inspired from Wu et al.'s study. As in the most of image processing studies based SNN, the network structure has three layer: receptor layer, intermediate layer and output layer. Receptor layer comprises of photoreceptors related to each pixels of the image.

The intermediate layer is constituted with different types of neurons to obtain the receptive fields. The main difference of our study from the existing studies is in the receptive layer where neurons have synaptic connections. The receptive layer given in Figure 2 consists of four different receptive field (RF). In these

fields, gray level values are not directly used, instead the absolute difference between the gray level values of pixels shown with yellow and the gray level value of center pixel is utilized. Besides, the blue pixels are ignored and the gray level values of these pixels are taken as zero. These four different receptive field allow the determination of edges in different directions by making synaptic connections with four different neurons in the intermediate layer.

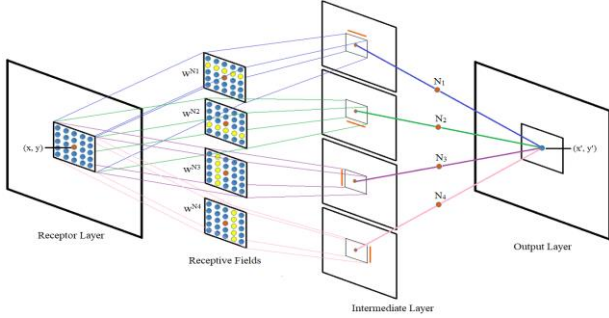


Figure 2. Proposed SNN structure

The output of these neurons was summed by each neuron in the output layer to obtain corresponding neuron's firing rate. Any direction edge within the input image can be obtained by means of the firing rates of the neurons at the output layer. To put a finer point on it, as shown from Figure 2, the preferred network model has four parallel arrays that have the same dimension with the receptor layer and have flagged as N_1 , N_2 , N_3 and N_4 for only one output neuron. These layers linked to receptor layer by changeable weight matrices help one to fulfill the processing of the edges (right, left, up and down). The size of these weight matrices can be changed by taking into consideration the receptive field's width. For instance, neuron N_1 links to the receptive field (RF) through a synaptic connection (w^{N1}) and gives an output if there is an edge. w^{N1} contains synapses which are enhances the membrane potential.

If all of the pixels within the RF have the same gray level value, the absolute value of the difference between the gray level values of the neighboring pixels and the gray level values of the center pixel will be 0. This will not change the membrane potential of neuron N_1 , thus neuron N_1 will not fire any spike. On the other hand, if the image in the RF has an upper edge, the N_1 will fire spike with the help of synaptic connections found just below the center.

One can think that w^{N1} is like a filter that find the upper-edge within the receptive field. Similarly, within the receptive field, the down-edge can be detected by neuron N_2 with the synaptic matrix with w^{N2} ; the left-edge can be detected by neuron N_3 with the synaptic matrix with w^{N3} ; and the right-edge can be detected by neuron N_4 with the synaptic matrix with w^{N4} . Finally, the neuron in the output layer sums the all of the outputs of these neurons at the intermediate layer and can elicit any direction edge within the receptive fields (RFs). This section may be

divided by subheadings. It should provide a concise and precise description of the experimental results, their interpretation as well as the experimental conclusions that can be drawn.

As stated before, the conductance based IF neuron model is simple and easy to analyze as compared with HH neuron model. Therefore, aforementioned network model is carried out based on conductance based IF neuron model. In the model, (x, y) represents the pixel coordinate in the RFs and each pixel in RFs can be defined as the absolute difference of gray level values ($G_{x,y}$). For the receptive fields peak conductance value of each pixel is calculated by the following expressions.

$$R_{x,y} = |G_{x,y} - G_{x_c,y_c}| \quad (2)$$

$$q_{x,y} = \alpha R_{x,y} \quad (3)$$

where G_{x_c,y_c} is the gray level value of the center pixel in RFs, $R_{x,y}$ is the absolute difference of center pixel gray level G_{x_c,y_c} and its neighbor pixel gray level $G_{x,y}$. $q_{x,y}$ is the peak conductance and α is the normalization coefficient.

Since the synaptic connections are based on the absolute difference between the gray level values, the peak synaptic conductance value of a neighboring pixel having the same value with the center pixel will be 0 (zero). Hence, the all-synaptic connections have been assumed as excitatory synapse. When all the pixels in the RFs had the same value, there would not be found any spike because all of the peak conductance would be equal zero.

For a neuron in the intermediate layer (e.g. N_1), the following equations are given:

$$\frac{dg_{x,y}^{syn}(t)}{dt} = -\frac{1}{\tau_{syn}} g_{x,y}^{syn}(t) + q_{x,y} \quad (4)$$

$$c_m \frac{dv_{N1}(t)}{dt} = g_l (E_l - v_{N1}(t)) + \sum_{(x,y) \in RF_1} \frac{w_{x,y}^{N1}(t) g_{x,y}^{syn}(t)}{A_{syn}} (E_{syn} - v_{N1}(t)) \quad (5)$$

Where c_m is the membrane capacitance, g_l represents the membrane conductance and E_l is reversal potential of the membrane. E_{syn} is the reversal potential of the synapses connected to RF1. $g_{x,y}^{syn}$ represents the conductance of the synapse corresponding to the pixel in RF and A_{syn} is the membrane patch area connected to the synapse. $w_{x,y}^{N1}$ shows the weight of the synapses and calculates as:

$$w_{x,y}^{N1} = \begin{cases} 0 & \text{if } (y - y_c) \neq 1 \\ w_{max} e^{-\frac{(x-x_c)^2}{\delta_x} - \frac{(y-y_c)^2}{\delta_y}} & \text{if } (y - y_c) = 1 \end{cases} \quad (6)$$

Where (x_c, y_c) gives the center of the RF_1 , (δ_x, δ_y) are constants and w_{max} are the maximum weight for synapses. Similarly, these equations are also valid and should be calculated for other neurons at the intermediate layer (that is N_2, N_3, N_4). If $v(t)$ reaches a certain threshold v_{th} (spiking threshold), it is instantaneously reset to a lower value v_r (reset potential) for a time τ_{ref} (refractory time) and a spike occurs. Let $S_{Ni}(t)$ gives a spike train, which is fired by neuron i ;

$$S_{Ni}(t) = \begin{cases} 1 & \text{if neuron } i \text{ fires a spike at time } t \\ 0 & \text{if there is no spike at time } t \end{cases} \quad (7)$$

Finally, each neuron in the output layer ($N(x', y')$) is defined by the following equations [19]:

$$\frac{g_{x',y'}^{syn}(t)}{dt} = -\frac{1}{\tau_{syn}} g_{x',y'}^{syn}(t) + (w_{N1}S_{N1}(t) + w_{N2}S_{N2}(t) + w_{N3}S_{N3}(t) + w_{N4}S_{N4}(t)) \quad (8)$$

$$c_m \frac{dv_{x',y'}(t)}{dt} = g_l (E_l - v_{x',y'}(t)) + \frac{g_{x',y'}^{syn}(t)}{A_{syn}} (E_{syn} - v_{x',y'}(t)) \quad (9)$$

It should be noted that each neuron at the output layer is linked to intermediate neuron merely by excitatory synapses.

3. Results and Discussion

The proposed model was performed in MATLAB using the following parameters: $v_{th} = -60 mV$, $v_{reset} = -70 mV$, $E_{syn} = 0$, $E_l = -70 mV$, $g_l = 1 \mu S mm^2$, $c_m = 10 nF mm^2$, $\tau_{syn} = 4 ms$, $\tau_{ref} = 6 ms$ and $A_{ex} = 0.028953 mm^2$. The strength of the synapses are adjusted by the maximal weights relevant synapses to guarantee that the neuron does not fire if the input image has a uniform structure. w_{max} is taken as 0.7093. The absolute differences of gray level values are set to be in the range of 0 to 1. To do this, α is determined by $1/255$. $\delta_x = 6$, $\delta_y = 2$, and the width and height of the RFs are set to 5. The matrices used for $w_{x,y}^{N1}$ and $w_{x,y}^{N2}$ are given as follows:

The edges of the original image shown in Figure 3 are determined with the preferred model and the result is shown as a gray level image. Firing rates of each $N(x', y')$ neuron in the output layer are used as gray level values. The value of the gray level approaches to 255, i.e. to white, at high firing rate pixels; whereas at low firing rate pixels, its values are 0, i.e. black. The preferred model was tested using 200 images on BSDS dataset and the results were calculated as F-scores. The F-score is the harmonic mean of the precision and recall values. The precision value is the ratio of the true edge pixels in all selected edge pixels by algorithm and recall is the ratio of the edge pixels selected by algorithm in image. The results were

compared with the Canny edge detector known as the most common edge detection method.

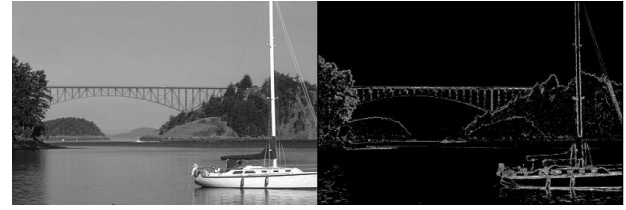


Figure 3. The result of the edge detection

In Figure 4, the first row shows 3 images in BSDS Train dataset. The edges of these images that are determined by the users manually are displayed at the second row of the figure. The results, which were determined by using the proposed model and Candy edge detection method, are given in the third and fourth rows of the figure, respectively. Both of these methods are quite successful for these images. The success of the proposed model as F-score were 0.7681, 0.7369 and 0.9536 by column order, whereas the success of the Candy edge detection method was obtained 0.7372, 0.7135 and 0.9542, respectively.

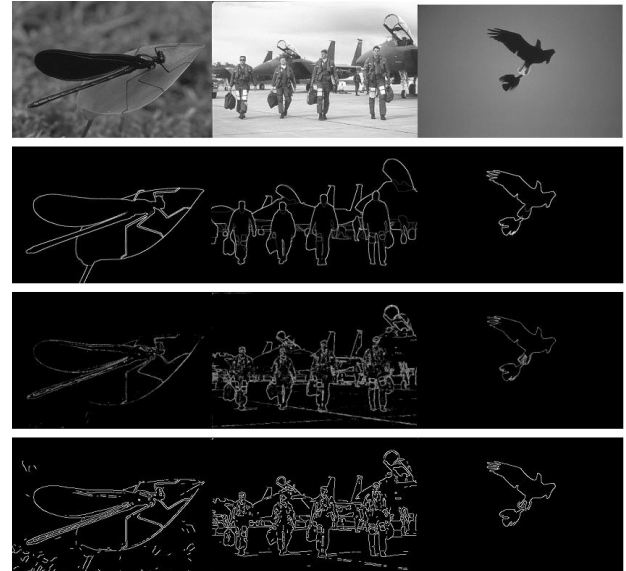


Figure 4. Edge detection results. Original images (1st row), ground truth edges (2nd row), results of proposed method (3rd row), canny results (4th row)

Figure 5 shows the results obtained for 2 different sample images. The first column is the original images in the BSDS Train dataset, whereas the grand truth images of them is given in the second column. The results obtained from the proposed model and Candy edge detection method are presented in the third and fourth columns, respectively. The recall, precision and F-score values of the proposed model for the face image in the first row of Figure 5, respectively, are 0.7773, 0.7332 and 0.7546, while these values are calculated as 0.8689, 0.7890 and 0.8271 by the Candy edge detection method. The image in the second row is the image in which the worst results are obtained by these two methods. The recall, precision and F-score values for this image

calculated by proposed model are 0.6006, 0.0955 and 0.1648, whereas they are computed as 0.8718, 0.0864 and 0.1572 by Canny edge detection method.



Figure 5. Examples of edge detection results. Original images (1st col), ground truth edges (2nd col), results of proposed method (3rd col), canny results (4th col)

Table 1 depicts the average values of the edge detection results of all images. It is seen that F-score values obtained from both methods are quite close to each other. But the recall values obtained with the canny edge detection method are higher as seen from the average values. These shows that Canny edge detection method is more successful to find the right edges. On the other hand, the precision values obtained with the proposed model are higher than the values calculated by the Canny edge detection method. This shows that the proposed method produces more successful results in terms of pixels accidentally marked as an edge.

Table 1. Average Results.

Edge Detection Methods	Recall	Precesion	F-score
Canny	0.8013	0.4344	0.5357
Proposed model	0.6876	0.4766	0.5381

4. Conclusion

Although SNNs are used for edge detection, it is seen that there are very few studies in the literature. SNNs, which can work similarly to human visual system, are still used with different designs. In this study, a new edge detection technique based on SNN is presented. The proposed model is tested on 200 image in the BSDS train dataset. Besides, canny edge detection method, which is one of the most known method for edge detection, is used on the same images for comparison. The F-score values are calculated for all of them. In addition, this is the first that the results are given as f-score in the edge detection studies using SNNs. It is observed that there are major differences in Recall and precision values obtained by proposed method and Canny edge detection method,

although there is a slight difference in the calculated F-score values. For this reason, it is planned to make changes on the network structure in order to increase the Recall values in future studies.

References

- [1] Canny, J. A. 1986. Computational Approach to Edge-detection. *IEEE Transactions on Pattern Analysis and Machine Intelligence*, 8(6), 679-698.
- [2] Demirci, R. 2007. Similarity Relation Matrix-Based Color Edge Detection. *AEU-International Journal of Electronics and Communications*, 61(7), 469-477.
- [3] Gonzalez, R.C., Woods, R.E. 2008. *Digital Image Processing*, 3rd Ed. Pearson/Prentice Hall, New Jersey.
- [4] Wandell, B. A. 1995. *Foundations of Vision*. Sinauer Associates, Inc., Sunderland, MA, 476s.
- [5] Kaiser, P. K., Boynton, R. 1996. *Human Color Vision*, 2nd edition. Optical Society of America, Washington, DC, 652s.
- [6] Nadenau, M.J., Winkler, S., Alleysson, D., Kunt, M., 2000. Human vision models for perceptually optimized image processing—a review. *Proceedings of the IEEE*, 32.
- [7] Kerr, D., Mcginnity, T.M., Coleman, S., Clogenson, M. 2015. A Biologically Inspired Spiking Model of Visual Processing for Image Feature Detection. *Neurocomputing*, 158, 268-280.
- [8] Kandel, E. R., Schwartz, J. H., Jessell, T. M. 2000. *Principles of Neural Science*. 4nd edition, McGraw-Hill, New York, 1760s.
- [9] Hosoya, T., Baccus, S. A., Meister, M. 2005. Dynamic Predictive Coding by the Retina. *Nature*, 436, 71 – 77.
- [10] Wu, Q., McGinnity, M., Maguire, L., Belatreche, A., Glackin, B., 2007, August. Edge detection based on spiking neural network model. In *International Conference on Intelligent Computing* (pp. 26-34). Springer, Berlin, Heidelberg.
- [11] DiCarlo, J., Zoccolan, D., Rust, N.C. 2012. How does the Brain Solve Visual Object Recognition? *Neuron* 73(3), 415–434.
- [12] Clarke, A., Tyler, L.K., 2015. Understanding what we see: how we derive meaning from vision. *Trends in cognitive sciences*, 19(11), 677-687.
- [13] Ghahari, A., Enderle, J. D. 2015 *Models of Horizontal Eye Movements: Part4, A Multiscale Neuron and Muscle Fiber-Based Linear Saccade Model*. Synthesis Lectures on Biomedical Engineering, Morgan & Claypool Publishers.
- [14] Kunkle, D. R., Merrigan, C. 2002. *Pulsed Neural Networks and Their Application*. Computer Science Dept., College of Computing and

- Information Sciences, Rochester Institute of Technology.
- [15] Ghosh-Dastidar, S., Adeli, H., 2009. Spiking neural networks. *International journal of neural systems*, 19(04), 295-308.
- [16] Ponulak, F. and Kasinski, A., 2011. Introduction to spiking neural networks: Information processing, learning and applications. *Acta neurobiologiae experimentalis*, 71(4), 409-433.
- [17] Rozenberg, G., Bäck, T., Kok, J. N. 2011. *Handbook of Natural Computing*. Springer, Berlin, 2052s.
- [18] Yedjour, H., Meftah, B., Lézoray, O., Benyettou, A., 2017. Edge detection based on Hodgkin-Huxley neuron model simulation. *Cognitive processing*, 18(3), 315-323.
- [19] Wu, Q., McGinnity, M., Maguire, L., Glackin, B., Belatreche, A., 2007. Learning mechanisms in networks of spiking neurons. In *Trends in Neural Computation* (pp. 171-197). Springer, Berlin, Heidelberg.
- [20] Meftah, B., Lezoray, O., Benyettou, A., 2010. Segmentation and edge detection based on spiking neural network model. *Neural Processing Letters*, 32(2), 131-146.
- [21] Kerr, D., Coleman, S., McGinnity, M., Wu, Q. X., Clongson, M. 2011. Biologically Inspired Edge Detection. 11th International Conference on Intelligent Systems Design and Applications, 22-24 November, Cordoba, Spain.
- [22] Díaz-Pernas, F.J., Antón-Rodríguez, M., de la Torre-Díez, I., Martínez-Zarzuela, M., González-Ortega, D., Boto-Giralda, D., Díez-Higuera, J.F., 2011. Surround suppression and recurrent interactions V1-V2 for natural scene boundary detection. *Image segmentation*. INTECH Publisher, pp.99-118.
- [23] Azzopardi, G., Petkov, N., 2012. A CORF computational model of a simple cell that relies on LGN input outperforms the Gabor function model. *Biological cybernetics*, 106(3), 177-189.
- [24] Hodgkin, A.L., Huxley, A.F., 1952. A quantitative description of membrane current and its application to conduction and excitation in nerve. *The Journal of physiology*, 117(4), 500-544.
- [25] Nelson, M. E., 2004. *Electrophysiological Models*. Koslow, S., Subramaniam, S., (Eds.) In *Data Basing the Brain: From Data To Knowledge*. Wiley, New York, 480s.
- [26] FitzHugh, R. 1969. *Mathematical Models of Excitation and Propagation in Nerve*. McGraw Hill, New York.
- [27] Nagumo, J., Sato, S. 1972. On a Response Characteristic of Mathematical Neuron Model. *Kybernetik*, 10(3), 155-164.
- [28] Gerstner, W., Kistler, W. M. 2002. *Spiking Neuron Models: Single Neurons, Populations, Plasticity*. Cambridge Univ. Press, United Kingdom, 496s.
- [29] Izhikevich, E. M. 2003. Simple Model of Spiking Neurons. *IEEE Trans. Neural Networks*, 14, 1569-1572.
- [30] Maass, W., Bishop, C. M. 1999. *Pulsed Neural Networks*. MIT Press, Cambridge, MA, 377s.
- [31] Richardson, M. J. E., Gerstner, W. 2003. Conductance Versus Current-Based Integrate-and-Fire Neurons: Is There Qualitatively New Behaviour? *Lausanne lecture*.
- [32] Mainen, Z. F. 1995. Mechanisms of spike generation in neocortical neurons. University of California, Doctoral dissertation, 72s, San Diego.
- [33] Destexhe, A., 1997. Conductance-based integrate-and-fire models. *Neural Computation*, 9(3), 503-514.
- [34] Koch, C. 1999. *Biophysics of Computation: Information Processing in Single Neurons*. Oxford University Press, New York, 588s.
- [35] Dayan, P., Abbott, L. F. 2001. *Theoretical Neuroscience: Computational and Mathematical Modeling of Neural Systems*. The MIT Press, Cambridge, 480s.
- [36] Müller, E. 2003. Simulation of high-conductance states in cortical neural networks. University of Heidelberg, Master's Thesis, Germany, 41s.